# Diagrams of stability of circumbinary planetary systems

E.A. Popova
Pulkovo Observatory of the Russian Academy of Sciences

*The stability diagrams in the "pericentric distance — eccentricity" plane of initial data are built and analyzed for Kepler-38, Kepler-47, and Kepler-64 (PH1). This completes a survey of stability of known up to now circumbinary planetary systems, initiated in Ref. [1], where the analysis was performed for Kepler-16, 34, and 35. In the diagrams, the planets appear to be "embedded" in the fractal chaos border; however, I make an attempt to measure the "distance" to the chaos border in a physically consistent way. The obtained distances are compared to those given by the widely used numerical-experimental criterion by Holman and Wiegert [2], who employed smooth polynomial approximations to describe the border. I identify the resonance cells, hosting the planets.*

## Introduction

There are more than 80 exoplanets discovered in the binary stellar systems [3]. They constitute two types: P-type planets, orbiting about the binary barycenter, and S-type planets, orbiting around one of the two stars. In total, 17 exoplanets belong to the type P, 8 of them orbiting around binaries, composed of main sequence stars (Kepler-16, 34, 35, 38, 47, 64, and 413). Welsh et al. [4] review all these systems except Kepler-413. The systems Kepler-16, 34, and 35 were considered in Ref. [1]: stability diagrams were constructed in the plane of initial parameters "pericentric distance — eccentricity", which showed that all three planets are situated in resonance cells bounded by unstable resonances. Here we consider the planetary dynamics in the systems Kepler-38, 47, and 64. The parameters of the systems are given in Table 1, compiled on the basis of the data contained in Refs. [5, 6, 7].

| | Kepler-38 | Kepler-47(b) | Kepler-64 |
|---|---|---|---|
| $m_{\rm A}$, $M_\odot$ | 0.949 | 1.043 | 1.14 |
| $m_{\rm B}$, $M_\odot$ | 0.249 | 0.362 | 0.28 |
| $a_{\rm s}$,, AU | 0.1469 | 0.0836 | 0.1622 |
| $e_{\rm s}$ | 0.1032 | 0.0234 | 0.2207 |
| $T_{\rm s}$, d | 18.795 | 7.448 | 20.000 |
| Spectral class (A) | G | G | F |
| Spectral class (B) | M | M | M |
| $m_{\rm p}$, $M_{\rm J}$ | 0.384 | 0.27 | 0.53 |
| $a_{\rm p}$, AU | 0.4644 | 0.2956 | 0.5644 |
| $e_{\rm p}$ | $< 0.032$ | $< 0.035$ | $< 0.09$ |
| $T_{\rm p}$, d | 105.595 | 49.514 | 137.82 |

Tab. 1 : Parameters of the systems

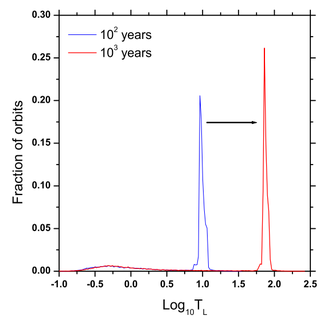


Fig. 1 : The differential distribution of the Lyapunov time logarithm for Kepler-47

## Methods

To explore the stability problem for the planetary motion, we use two stability criteria, following Ref. [1]. The first one is the "escape-collision" criterion: the orbit is stable if the distance between the planet and one of the stars does not become less than a star radius or does not exceed 100 AU. The second criterion is based on the value of the maximum Lyapunov characteristic exponent (maximum LCE).

The computations are performed using the algorithms and codes [8, 9, 10, 11]. The LCE spectra are obtained for each point on a grid of the initial data. Differential distributions of the maximum LCE are calculated on two different time intervals in order to separate the chaotic and regular orbits. This statistical method for separation of regular and chaotic orbits was proposed in Refs. [12, 13]. It consists of 4 steps: (1) Two differential distributions of the maximum LCE are constructed for the initial data grid using two different integration time intervals. Thus one obtains two differential distributions of the maximum LCE. (2) Each of these distributions has at least two peaks. The peak that shifts (moves in the direction of smaller values), when the integration time interval is increased, corresponds to the regular trajectories. (3) The maximum LCE value in the middle between the peaks gives the numerical criterion for separation of regular and chaotic trajectories. (4) In further computations on finer initial data grids, the obtained criterion can be used to separate regular and chaotic trajectories using relatively small time intervals of integration. An example of obtaining the criterion value is given in Fig. 1.

## Chaos border

Holman and Wiegert [2] obtained an empirical formula for the critical semimajor axis (separating the chaotic and regular domains) in function of the binary mass ratio and the binary eccentricity, for zero eccentricity planetary orbits:

$$\frac{a_{\rm cr}}{a_{\rm s}} = (1.60 \pm 0.04) + (5.10 \pm 0.05)e_{\rm s} + (-2.22 \pm 0.11)e_{\rm s}^2 + (4.12 \pm 0.09)\mu + \\ + (-4.27 \pm 0.17)e_{\rm s}\mu + (-5.09 \pm 0.11)\mu^2 + (4.61 \pm 0.36)e_{\rm s}^2\mu^2,$$

where $a_{\rm s}$ and $e_{\rm s}$ are the semimajor axis and eccentricity of the binary, $\mu = m_2/(m_1 + m_2)$, and $m_2 < m_1$ are the masses of the binary components.

In Table 2, columns 2 and 3 give the semimajor axes of the binary and planet orbits, respectively. The Holman–Wiegert $a_{\rm cr}$ values are given in column 4, whereas our numerical estimates $a'_{\rm cr}$ (the main border at zero eccentricity; it is provided by the stability diagrams) are given in column 5. Column 6 gives the ratio of these two values. The nearest-to-planet semimajor axis values $a'_{\rm ncr}$, corresponding to the orbits unstable by the LCE criterion, are given in column 7. Column 8 gives the real distance "planet — chaos border".

| | $a_{\rm s}$, AU | $a_{\rm p}$, AU | $a_{\rm cr}$, AU | $a'_{\rm cr}$, AU | $a'_{\rm cr}/a_{\rm cr}$ | $a'_{\rm ncr}$, AU | $a_{\rm p} - a'_{\rm ncr}$, AU |
|---|---|---|---|---|---|---|---|
| Kepler-16b | 0.224 | 0.705 | 0.646 | 0.619 | 0.958 | 0.667 | 0.038 |
| Kepler-34b | 0.229 | 1.090 | 0.836 | 0.755 | 0.903 | 1.079 | 0.011 |
| Kepler-35b | 0.176 | 0.603 | 0.497 | 0.481 | 0.968 | 0.594 | 0.009 |
| Kepler-38b | 0.147 | 0.464 | 0.389 | 0.395 | 1.015 | 0.444 | 0.020 |
| Kepler-47b | 0.084 | 0.296 | 0.202 | 0.178 | 0.881 | 0.280 | 0.016 |
| Kepler-64b | 0.162 | 0.564 | 0.495 | 0.434 | 0.877 | 0.542 | 0.022 |

Tab. 2 : Chaos border location

## Discussion

The computed stability diagrams for Kepler-38, 47, and 64 are given in Figs. 2 – 7. The chaotic domains revealed by the maximum LCE criterion are shown in blue, and those revealed by the "escape-collision" criterion are shown in green. Red dots are the nominal planet positions. As one can see, Kepler-38b is situated in the resonance cell between the "teeth" of instability corresponding to the resonances $5/1$ and $6/1$ between the orbital periods of the planet and binary. The planet orbit lies close to the half-integer resonance $11/2$. The representative value of the Lyapunov time in the chaos domain is $\sim 1.5$ years. Kepler-47b is close to the half-integer resonance $13/2$, situated between the unstable resonances $6/1$ and $7/1$, and the Lyapunov time in the chaos domain is $\sim 1$ year. Kepler-64b is as well situated in the resonance cell formed by the $6/1$ and $7/1$ resonances (this is consistent with findings by Kostov et al. [7]), and the Lyapunov time in the chaos domain is $\sim 1$ year, as in the case of Kepler-47b. Thus all the circumbinary planets are "embedded" in the fractal chaos border in the stability diagrams.

## Stability diagrams

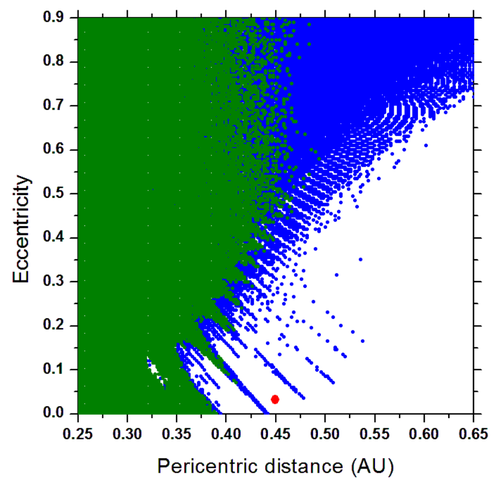


Fig. 2 : The stability diagram for Kepler-38

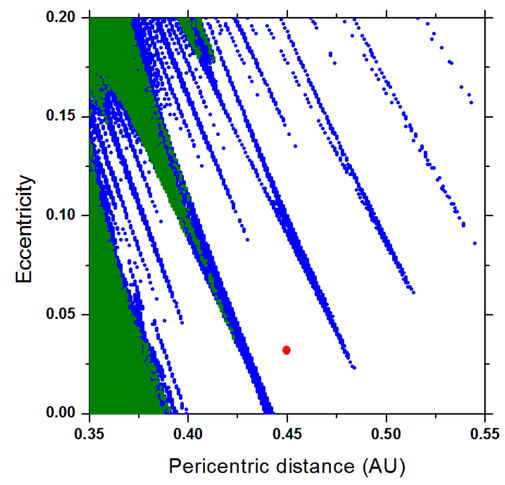


Fig. 3 : Zoom of the stability diagram for Kepler-38

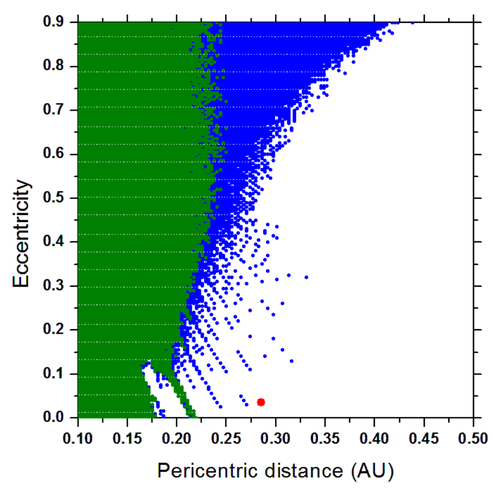


Fig. 4 : The stability diagram for Kepler-47

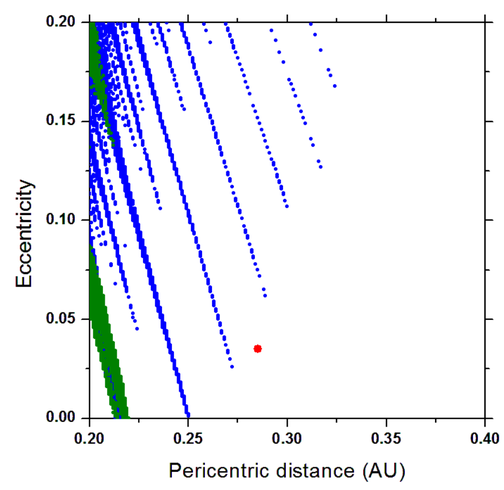


Fig. 5 : Zoom of the stability diagram for Kepler-47

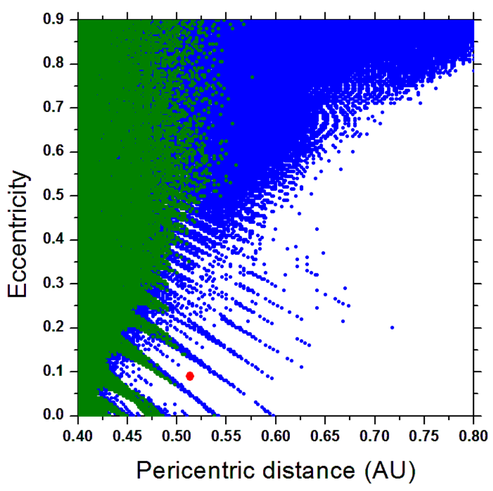


Fig. 6 : The stability diagram for Kepler-64

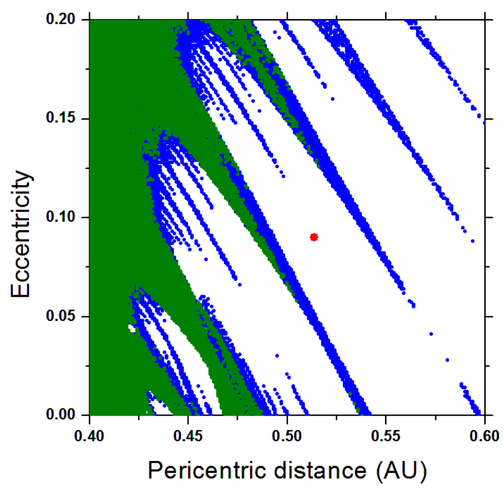


Fig. 7 : Zoom of the stability diagram for Kepler-64

## Conclusions

• The stability diagrams in the "pericentric distance — eccentricity" plane of the initial data have been built for Kepler-38, 47, and 64. In these diagrams, the planets turn out to be situated in resonance cells at the fractal chaos border, similar to the planets Kepler-16b, 34b, and 35b, considered in Ref. [1]. Thus all the circumbinary planets are "embedded" in the fractal chaos border in the stability diagrams.

• The semimajor axis critical values, given by the Holman–Wiegert empirical criterion, may differ significantly from real ones (directly obtained from the stability diagrams). The measured distances between the planet locations and the nearest unstable resonant "teeth" do not exceed $6\%$ of the planet semimajor axes.

• The representative values of the Lyapunov time in the chaotic domains for the studied planets are very small: 1–1.5 years.

## References

[1] E.A. Popova, I.I. Shevchenko, Astrophys. J., **769**, 152 (2013)
[2] M. J. Holman, P. A. Wiegert, Astron. J., **117**, 621 (1999)
[3] Exoplanet Encyclopedia, http://www.exoplanet.eu/
[4] W.F. Welsh et al., Proceedings of the IAU, IAU Symposium 293, **8**, 125 (2014)
[5] J. Orosz, W. Welsh, J. Carter et al., Astrophys. J., **758**, 82 (2012)
[6] J. Orosz, W. Welsh, J. Carter et al., Science, **337**, 1511 (2012)
[7] V.B. Kostov et al., Astrophys. J., **770**, 52 (2013)
[8] H.F. von Bremen, F.E. Udwadia, W. Proskurowski, Physica D, **101**, 1 (1997)
[9] I.I. Shevchenko, V.V. Kouprianov, Astron. Astrophys., **394**, 663 (2002)
[10] V.V. Kouprianov, I.I. Shevchenko, Astron. Astrophys., **410**, 749 (2003)
[11] V.V. Kouprianov, I.I. Shevchenko, Icarus, **176**, 224 (2005)
[12] A.V.Melnikov, I.I. Shevchenko, Sol. Sys. Res., **32**, 480 (1998)
[13] I.I. Shevchenko, A.V.Melnikov, JETP Lett., **77**, 642 (2003)